MICROBIOLOGY

RESEARCH ARTICLE

Godoy-Santos *et al.*, *Microbiology* 2019;165:761–771

DOI 10.1099/mic.0.000804

Nisin penetration and efficacy against *Staphylococcus aureus* biofilms under continuous-flow conditions

Fernanda Godoy-Santos[1], Betsey Pitts[2], Philip S. Stewart[2,3] and Hilario C. Mantovani[1,*]

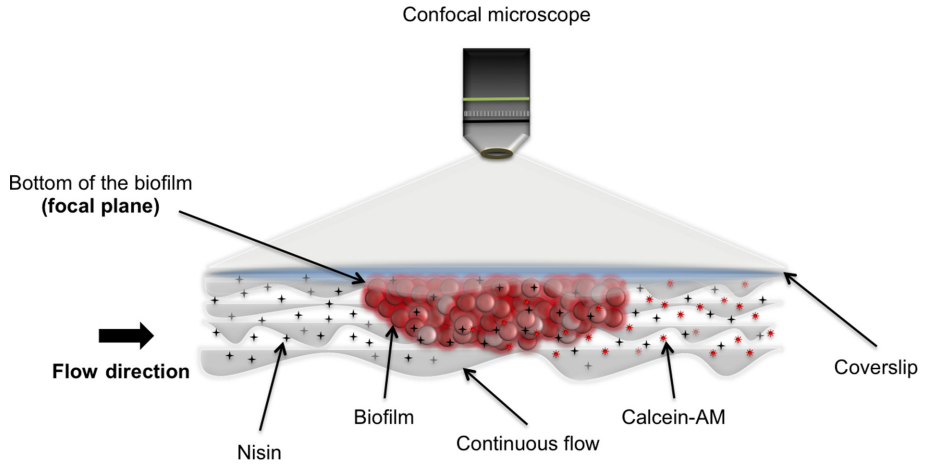

Graphical abstract

Abstract

Biofilms may enhance the tolerance of bacterial pathogens to disinfectants, biocides and other stressors by restricting the penetration of antimicrobials into the matrix-enclosed cell aggregates, which contributes to the recalcitrance of biofilm-associated infections. In this work, we performed real-time monitoring of the penetration of nisin into the interior of *Staphylococcus aureus* biofilms under continuous flow and compared the efficacy of this lantibiotic against planktonic and sessile cells of *S. aureus*. Biofilms were grown in Center for Disease Control (CDC) reactors and the spatial and temporal effects of nisin action on *S. aureus* cells were monitored by real-time confocal microscopy. Under continuous flow, nisin caused loss of membrane integrity of sessile cells and reached the bottom of the biofilms within ~20 min of exposure. Viability analysis using propidium iodide staining indicated that nisin was bactericidal against *S. aureus* biofilm cells. Time-kill assays showed that *S. aureus* viability reduced 6.71 and 1.64 log c.f.u. ml^{-1} for homogenized planktonic cells in exponential and stationary phase, respectively. For the homogenized and intact *S. aureus* CDC biofilms, mean viability decreased 1.25 and 0.50 log c.f.u. ml^{-1}, respectively. Our results demonstrate the kinetics of biofilm killing by nisin under continuous-flow conditions, and shows that alterations in the physiology of *S. aureus* cells contribute to variations in sensitivity to the lantibiotic. The approach developed here could be useful to evaluate the antibiofilm efficacy of other bacteriocins either independently or in combination with other antimicrobials.

INTRODUCTION

Staphylococcus aureus is a contagious opportunistic pathogen often associated with human and animal diseases such as mastitis, meningitis, skin and bloodstream infections [1, 2]. *S. aureus* infections are often characterized by a low rate of cure, high incidence and chronicity that contributes to its high impact on the public health and worldwide economy [3]. The chronicity and recalcitrance of these infections have been related to the ability of *S. aureus* to form biofilms, a complex mode of growth that contributes to the establishment and maintenance of persistent microbial infections [4, 5].

The nonspecific interactions between components of the biofilm matrix and antimicrobials pose the potential to retard diffusion of antimicrobial agents through the biofilm, reducing the efficacy of strategies that aim to control established biofilms [6]. This results in heterogeneous distribution

of inhibitors within the biofilm and the exposure of microbial cells to sublethal doses of the antimicrobials, selecting subpopulations of resistant cells [7] and increasing the incidence and persistence of bacterial infections [4, 8, 9].

In this context, bacteriocins of Gram-positive bacteria represent a potentially useful alternative to control clinical pathogens, such as methicillin-resistant *S. aureus* (MRSA), *Enterococcus faecalis, Listeria monocytogenes* and *Clostridium difficile* [10–12]. The lantibiotics are a subgroup of bacteriocins containing post-translationally modified amino acid residues (e.g. lanthionine and methyllanthionine amino acid residues). These molecules show a broad spectrum of activity and low cytotoxicity against mammalian cells, and have been studied for therapeutic applications [13, 14].

Nisin, an antimicrobial peptide that shows inhibitory activity in the nanomolar range against Gram-positive cells [15], is generally recognized as safe (GRAS) and has been used in more than 50 countries as a biopreservative for food products [16]. Nisin can bind lipid II with high affinity to form pores in the cytoplasmic membrane of target cells and also block peptidoglycan biosynthesis, thus inhibiting cell-wall formation [17]. As a consequence of having two distinct killing mechanisms, nisin kills planktonic bacteria quickly, and also shows bactericidal activity against biofilm cells [18].

Despite the clinical relevance of *S. aureus* as a pathogen for humans and animals, and that biofilm formation has been recognized as an important virulence factor in *S. aureus* [19], the temporal and spatial dynamics of nisin penetration into *S. aureus* biofilms has not been systematically addressed. Also, previous studies assessing the efficacy of nisin against bacterial biofilms were mostly based on static biofilm models that were not designed to monitor the diffusion/kinetics of bacteriocin penetration into the biofilm structure/matrix [11]. Therefore, investigating the penetration of nisin into the biofilm interior using different continuous-flow models could provide valuable insights about its kinetics of biofilm killing and/or removal, which is relevant for a deeper understanding of the mechanisms by which antimicrobials inhibit biofilm-associated infections. Also, the approach presented here can be useful to screen for antimicrobials with enhanced ability to diffuse through the complex structure of the bacterial biofilms as well as to evaluate the antibiofilm efficacy of other bacteriocins/lantibiotics either independently or in combination with other antimicrobials, potentially helping to improve antimicrobial dosing regimens [20].

In the present study, we investigated the behaviour of nisin penetration into the interior of *S. aureus* biofilms under continuous-flow conditions by monitoring diffusion with real-time confocal microscopy using a novel approach for biofilm visualization. Variations in the killing efficacy of nisin against *S. aureus* cells were related to alterations in the physiology of the bacteria and the capacity of the peptide to cause loss of membrane integrity on planktonic cells compared to matrix-enclosed bacterial cells.

METHODS

Micro-organism and growth conditions

S. aureus AH2547, a biofilm producer [21], was kindly provided by Alexander Horswill, University of Iowa (USA). *S. aureus* AH2547 contains the plasmid pCM29, which constitutively expresses a green fluorescent protein (GFP) and confers resistance to chloramphenicol. *S. aureus* AH2547 was cultivated overnight at 37 °C in 30 g.l^{-1} tryptic soy broth [TSB; Becton, Dickinson and Company (BD), Franklin Lakes, NJ, USA] supplemented with 10 ug ml^{-1} chloramphenicol (CHL, Fisher Scientific, Pittsburgh, PA, USA). Incubations were carried out in an orbital incubator at 200 r.p.m. To obtain exponential phase planktonic cultures, a 1 % (v/v) aliquot of an overnight culture was transferred to TSB media and incubated for 2 h.

Solutions and antimicrobial agents' stock solutions

The sodium phosphate buffer (PB, 100 µmol l^{-1}, pH 7.0) consisted of an aqueous solution containing, per litre, 4.57 g NaH_2PO_4 and 8.78 g Na_2HPO_4. Buffered dilution water used in the culture dilution procedures was composed of 0.0425 g l^{-1} KH_2PO_4 and 0.405 g l^{-1} $MgCl_2 6H_2O$ and was prepared according to Method 9050 C.1a [22]. Nisin stock solutions (2.5 % w/w; Sigma, N5764, Saint Louis, MO, USA) were prepared in PB and stored at 4 °C. Solution of 2-hydroxyethylagarose (4 % w/w; A4018-Sigma-Aldrich, Saint Louis, MO, USA) was prepared in distilled water, autoclaved for 10 min and stored at room temperature. Propidium iodide (PI, 20 µmol l^{-1}) was resuspended in ultrapure water. Film Tracer Calcein Red-Orange Biofilm Stain (CAM; F10319 Thermo Fisher Scientific, Waltham, MA, USA) was resuspended in

Received 23 January 2019; Accepted 30 March 2019; Published 14 May 2019
Author affiliations: [1]Departamento de Microbiologia, Universidade Federal de Viçosa, Viçosa, Minas Gerais, Brazil; [2]Center for Biofilm Engineering, Montana State University, Bozeman, Montana, USA; [3]Department of Chemical and Biological Engineering, Montana State University, Bozeman, Montana, USA.
*Correspondence: Hilario C. Mantovani, hcm6@ufv.br
Keywords: TL-CLSM; PI staining; Calcein-AM; CDC biofilms; Antimicrobial peptides; Continuous-flow biofilm.
Abbreviations: CAM, calcein red-orange; CDC, Center for Disease Control; eDNA, extracellular nucleic acid; GFP, green fluorescent protein; GRAS, Generally Recognized as Safe; HB, homogenized biofilms; HEP, homogenized exponential planktonic cells; HSP, homogenized stationary planktonic cells; IB, intact biofilms; MIC, minimum inhibitory concentration; MRSA, methicillin-resistant *S. aureus*; PB, sodium phosphate buffer; PI, propidium iodide; QAC, quaternary ammonium compounds; TL-CLSM, time-lapse confocal laser scanning microscopy.
Three supplementary figures and six supplementary movies are available with the online version of this article.

DMSO at final concentration of 0.416 ug ml^{-1}. Both dye solutions were stored at −20 °C until use.

MIC

MIC of nisin was determined by the Clinical and Laboratory Standards Institute micro-broth dilution method [23]. The nisin concentration range tested varied from 0.1 to 12.5 µmol l^{-1}. The MIC was defined after 48 h of incubation at 37 °C. Results represent the mean values of two independent determinations performed with three technical replicates.

Calcein-AM (CAM) staining

Overnight planktonic cultures were centrifuged and resuspended in 1 ml of sterile water. Cell suspensions were stained with 20 µl of CAM stock solution for 1 h at room temperature. Excess CAM was removed by centrifugation. Similarly, Center for Disease Control (CDC) coverslip biofilms were immersed into 2.5 ml PB added with 50 µl of CAM stock solution. Excess CAM was removed by rinsing with PB.

Nisin effect on cytoplasmic calcein retention

CAM-stained overnight planktonic cultures were exposed to 15 or 150 µmol l^{-1} of nisin for 60 min at room temperature. The control treatment was performed using PB without nisin. Samples were immobilized by filtration (Lab System 3 – Millipore Corporation, Bedford, MA, USA), onto polycarbonate black membranes (25 mm, 0.22 µM pore size, Osmonics INC, Minnetonka, MN, USA) and transferred to glass slides (Fisherbrand Superfrost/Plus microscope slides, Fisher Scientific, Pittsburgh, PA, USA). Samples were examined microscopically.

Artificial coverslip biofilm

CAM-stained overnight planktonic cultures were transferred to a 4 % solution of 2-hydroxyethylagarose at 50±5 °C with a 1:1 proportion. The mixture was vortexed and small drops were dispensed onto circular glass coverslips (Fig. 1a; 1.5 Micro Cover Glass-72225–01; Electron Microscopy Sciences, Hatfield, PA, USA).

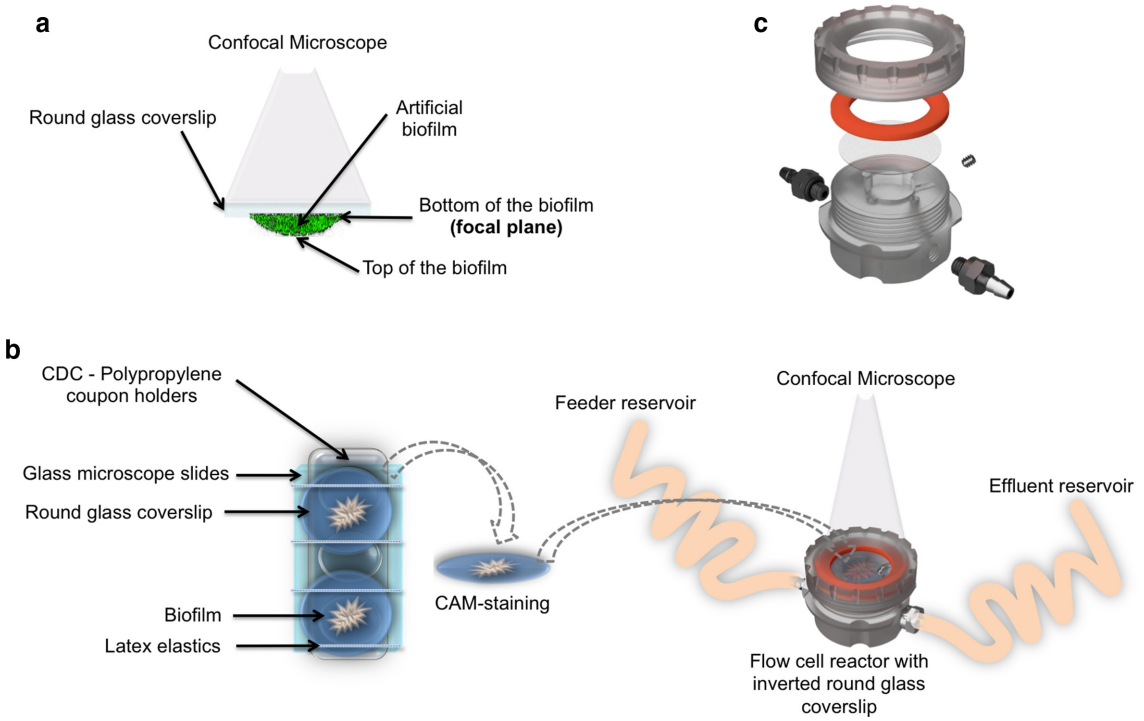

Fig. 1. Schematic representation of flow cell device and experimental steps to obtain and treat CDC coverslip biofilms with nisin under flow conditions. (a) General view of the artificial coverslip biofilm with indication of the target focal plane used in the flow treatments. (b) *S. aureus* biofilms were grown in a CDC reactor containing round glass coverslips fastened to microscope slides with rubber bands. The CDC coverslips containing *S. aureus* biofilms were removed from the CDC reactor and then stained with CAM. The inverted glass coverslip containing the biofilm was placed in a flow cell reactor as indicated in the scheme. A solution of 15 µmol l^{-1} nisin was supplied from the feeder reservoir to the flow cell at a rate of 2 ml min^{-1} during 1 h, at room temperature and the fluorescence at the bottom of the biofilm was monitored over time with a confocal microscope. PB without nisin was used as the control. (c) Components of the flow cell reactor used to treat artificial and CDC *S. aureus* biofilms with nisin (all right reserved to BioSurface Technologies Corporation). The flow cell reactor schematic drawings were reprinted from https://biofilms.biz/products/microscopy-flow-cells/treatment-imaging-flow-cell/ with permission of BioSurface Technologies Corporation, Bozeman, Montana, USA.

CDC biofilms

Sessile cultures were grown on glass coupons (12,7 mm diameter and 3,8 mm thickness) in CDC biofilm reactors (Biosurface Technologies, Bozeman, MT, USA) [24]. Briefly, 1 ml of an overnight planktonic culture was transferred to a reactor containing 400 ml of full-strength TSB media (30 g l^{-1}) and 10 ug ml^{-1} of chloramphenicol and incubated at 37 °C with constant stirring (125 r.p.m.). After 24 h, the continuous flow (11.7 ml min^{-1}) of one-tenth-strength TSB (3 g l^{-1}) was started and continued for 48 h. The outside surface (low shear side) of CDC coupons was used in biofilm experiments, and when appropriate, glass coverslips (25 mm diameter) were attached (Fig. 1b).

Flow cell reactor treatment and time-lapse confocal laser scanning microscopy (TL-CLSM) analysis

The flow cell reactor (Fig. 1c; Model FC 310 Treatment Imaging Flow Cell, BioSurface Technologies Corporation, Bozeman, Montana, USA) was placed on the stand of the microscope (CLSM) and connected to a peristaltic pump by silicone tubing connecting the feeder reservoir and the effluent reservoir (Fig. 1b). Glass coverslips containing CAM-stained artificial biofilms or CDC biofilms were placed, inverted, into the sterile flow cell reactor (volume of 0.500 mm^3), forming the cover. Next, the focus plane was adjusted. A solution of 15 µmol l^{-1} nisin was pumped at a rate of 2 ml per min for 1 h at room temperature (turnover time of approximately 15 s). PB without nisin addition was used as the control. Throughout the experiments, fluorescence intensities were monitored using bright field and fluorescence imaging on the confocal microscope, where six frames were recorded per second.

PI staining and cryosectioning of CDC biofilms

Biofilms were stained with PI as follows: 150 µl of stock PI solution were pipetted directly onto the biofilm surface and the coupons were allowed to sit for 10 min at room temperature. Excess PI was gently removed by rinsing with sterile water. Biofilm samples were frozen using Tissue-Tek O.C.T. compound (Miles Laboratories, Elkhart, Indiana, USA), as described previously [25]. Samples without PI staining were used as controls.

Microscopy analyses

Epi-fluorescent images were captured on a Nikon Eclipse E-800 microscope using a Photometrics CoolSNAP MYO CCD camera and MetaVue software (Universal Imaging, Downingtown, PA, USA). Standard FITC and TRITC fluorescence filter cubes were used to visualize the GFP fluorescence (green fluorescence) and PI/Calcein fluorescence (red fluorescence), respectively, with a 20×0.75 NA dry objective. Confocal images were acquired using a Leica TCS-SP5 confocal scanning laser microscope (CSLM), with ×10 objective lens. The 488 nm and 561 lasers were used for excitation of fluorophores, and the detector bandwidth was set to collect GFP and calcein emission fluorescence between 500–550 nm and 575–675 nm, respectively. The fluorescence intensity was measured using Metamorph and Imaris software (Bitplane Scientific Software, Saint Paul, MN, USA). Twelve regions measuring 10 μm^2 each and representing different fields of view of the *S. aureus* biofilms (e.g. center, middle and edge zone for the CDC artificial biofilms or the biofilm cluster center in the CDC coupons) were selected for microscopy analysis, as fluorescence could vary across different regions of the biofilm (Fig. S1, available in the online version of this article). A single plane of focus for each sample was selected and the GFP and calcein fluorescence intensities were measured during the treatment. Background fluorescence was subtracted from the final values. The fluorescence values were normalized as relative intensity by dividing the values of GFP intensity by calcein intensity at that specific location.

Nisin susceptibility of homogeneous cultures

Planktonic cultures were centrifuged (2500 ***g***, 8 min at 4 °C), resuspended in buffered dilution water. The sessile cells were detached from the CDC coupon using a wooden scraper (see below) and resuspended in buffered dilution water. Both planktonic and sessile cultures were homogenized for 30 s (5000 r.p.m.; IKA T25 digital Ultra Turrax) at room temperature and the optical densities at 600 nm were standardized to 0.05. Aliquots of 1 ml from each culture were distributed in centrifuge microtubes and treated with 15 µmol l^{-1} nisin for 60 min at room temperature. PB without nisin was used as the control. Samples were removed at 0, 5, 15, 30 and 60 min after exposure to nisin. Additionally, cells were treated for up to 60 min with 150 µmol l^{-1} nisin. Samples were then washed by centrifugation (2500 ***g***, 8 min at 4 °C) to remove the antimicrobial and the cell pellets were resuspended in buffered dilution water. Serial dilutions were performed and 20 µl from each dilution were transferred onto TSA plates followed by incubation at 37 °C for 24 h [26].

Nisin susceptibility of CDC biofilms

S. aureus AH2547 biofilms were treated at room temperature with 150 µl of 15 µmol l^{-1} nisin, which covered the entire upper surface of the CDC coupon. PB without nisin was used as control. Samples were removed after 0, 5, 15, 30 and 60 min of nisin treatment, rinsed with the same volume of sterile buffered dilution water and the enumeration of viable cells on the CDC biofilm was performed as described below. When appropriated, biofilm samples were submitted to cryosection analyses as described above.

2.13. Viable cell count of CDC biofilms

Sessile cells were enumerated as previously described [24], with the modifications described below. Biofilm from the outward-facing side of the CDC coupon were scraped with a sterile wooden applicator stick. Each stick was rinsed and stirred into 10 ml of buffered dilution water. Solutions were homogenized for 30 s (5000 r.p.m.; IKA T25 digital Ultra Turrax) and serial dilutions were performed as previously described [26].

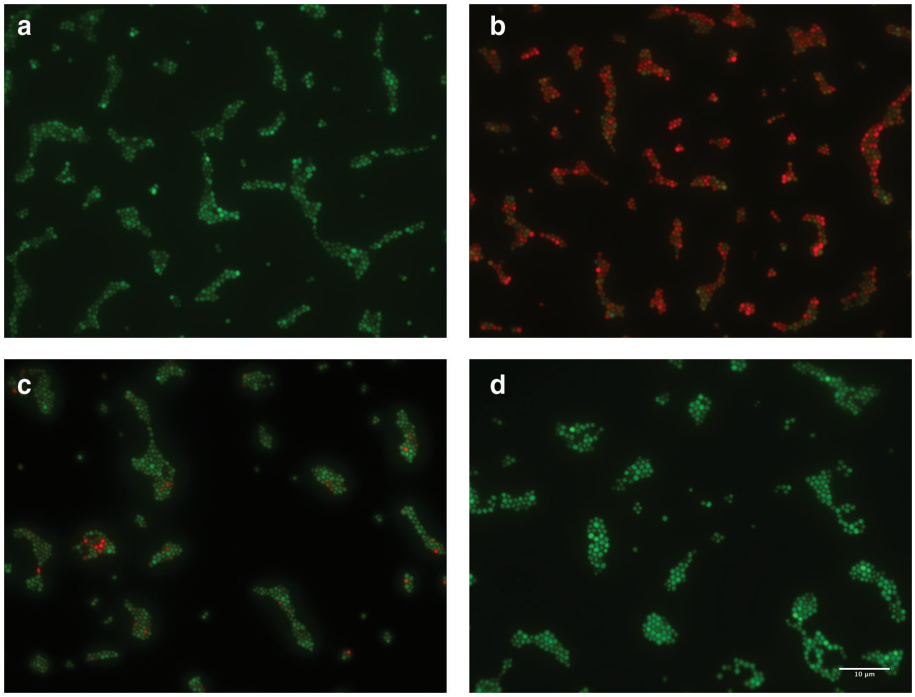

Fig. 2. Effect of nisin against CAM-stained cultures of *S. aureus* AH2547. Cell suspensions containing approximately 10^5 c.f.u. ml^{-1} of overnight planktonic *S. aureus* AH2547 were stained with CAM and incubated at room temperature with nisin (15 µmol l^{-1}) for 60 min. The cultures were immobilized onto black polycarbonate membranes and visualized by fluorescence microscopy (×100 magnification). (a) Culture not stained with CAM and exposed to nisin; (b) Culture stained with CAM and not exposed to nisin; (c) Culture stained with CAM and treated with 15 µmol l^{-1} nisin; (d) Culture stained with CAM and treated with 150 µmol l^{-1} nisin. Three independent evaluations were performed for each treatment and the images are representative of the observations fields for each treatment.

Statistical analysis

Statistical analysis was performed using GraphPad Prism (GraphPad Prism Software, San Diego, CA, USA). Significance of interaction effects between nisin and time of treatment was determined using a two-way repeated-measures ANOVA test. Post-hoc pairwise multiple comparison procedures included the Bonferroni test (comparing the mean of a treated group) and the Student–Newman–Keuls test (comparing the factor level mean within a treated group). Fluorescence ratio curves were compared using two-sample Kolmogorov–Smirnov tests. The probability level for statistical significance was $P<0.05$.

RESULTS

Broth dilution experiments showed that the MIC of nisin against *S. aureus* AH2547 was 1.56 mmol l^{-1}. To account for the physiological heterogeneity between planktonic and sessile cells and the increased resistance of biofilm-grown cells, subsequent killing assays were performed using 15 µmol l^{-1} (~10x MIC) or 150 µmol l^{-1} nisin (~100x MIC). To verify if nisin caused membrane permeabilization of target cells, overnight planktonic cultures of *S. aureus* AH2547 were stained with CAM (a fluorescent intracellular dye) and treated with nisin. The absence of red fluorescence was confirmed with cultures not stained with CAM but treated with nisin (Fig. 2a). Despite the fact that GFP produced by bacteria is sensitive to oxygen and susceptible to photobleaching, the *S. aureus* cultures fully retained their GFP fluorescence (green fluorescence) after nisin treatment, confirming that nisin does not cause significant loss of GFP fluorescence. Additionally, *S. aureus* cultures stained with CAM and treated with buffer without nisin retained most of their red fluorescence (Fig. 2b). However, cells stained with CAM and treated with nisin (15 µmol l^{-1}), showed an almost complete loss of intracellular calcein (Fig. 2c). This effect was even more dramatic when *S. aureus* cells were exposed to 150 µmol l^{-1} nisin (Fig. 2d). These results confirmed that calcein is a useful marker to monitor the antimicrobial activity of nisin on *S. aureus* cultures.

To adjust experimental conditions and to monitor the diffusion and activity of nisin under continuous-flow treatment, we developed an experimental approach to allow direct real-time evaluation of the bacterial biofilms treated with nisin. Stationary phase cultures were stained with CAM and immobilized in artificial coverslip biofilms made of agarose gels in a custom-made flow cell and fluorescence was monitored with TL-CLSM (Fig. 3). The artificial coverslip biofilms showed an average volume of 0.612 µl and thickness varying from approximately 660 µm in its center and 150 µm close to the border of the biofilm (Fig. S2). Both calcein and GFP fluorescence were consistently retained in untreated controls

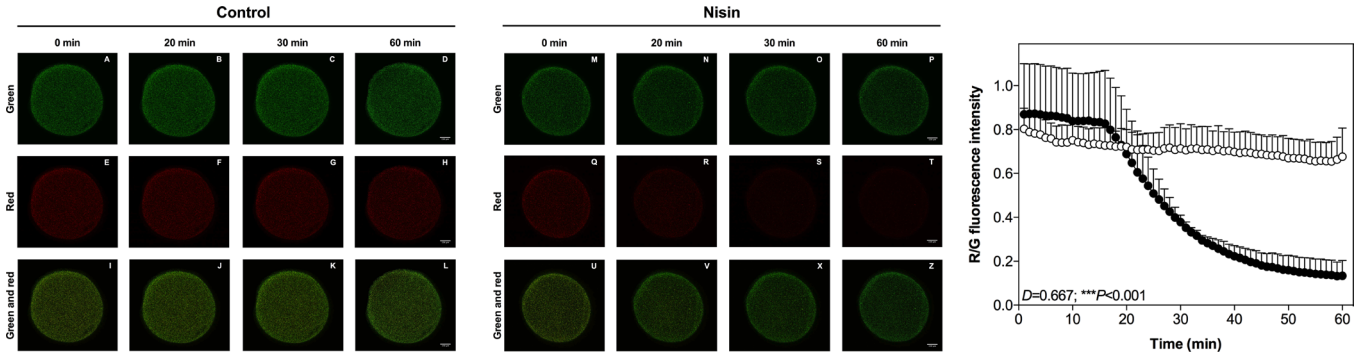

Fig. 3. Nisin flow cell treatment of *S. aureus* AH2547 artificial coverslip biofilms. Sequential images from GFP fluorescence (a-d, m–p), calcein fluorescence (e-h, q–t) and GFP and calcein-combined fluorescence (i–l, u–z) captured by TL-CSLM of *S. aureus* artificial coverslip biofilms under flow cell treatment in a rate of 2 ml min^{-1} at room temperature at 0, 20, 30 and 60 min. Control treatments were performed with phosphate buffer without nisin (a–l) and nisin treatment was performed with phosphate buffer with 15 µmol l^{-1} nisin (m–z). The focal plane in these experiments is located near the bottom of the artificial coverslip biofilms (the side close to the glass). The experiment was performed with three biological replicates and the images are representative for each treatment. Calcein to GFP fluorescence ratio from *S. aureus* artificial coverslip biofilms under flow cell reactor treatment were quantified using Metamorph software. Control treatment is shown in white circles and nisin treatment is shown in black circles. Fluorescence intensities were measured at 12 locations distributed randomly among the center, middle and edge zone of the biofilm. Data represent the means and sd of three replicates (only the upper limits of the error bars are represented). Calcein to GFP fluorescence ratio curves were compared by two-sample Kolmogorov–Smirnov tests (***P<0.001).

of the artificial coverslip biofilms, confirming minimal photobleaching and photodamage (Fig. 3a–l, Supplementary Movies 1 and 2). However, when artificial coverslip biofilms were treated with 15 µmol l^{-1} nisin, the red calcein fluorescence was progressively lost while the green GFP fluorescence was maintained over time, indicating extensive membrane permeabilization (Fig. 3m–z, Supplementary Movies, ,3 and 4). Variations in red fluorescence dissipation occurred at the edge and the center of the artificial biofilm (Fig. S3), while the GFP fluorescence remained unchanged.

S. aureus CDC coverslip biofilms were then submitted to flow cell reactor treatments similar to the ones applied for the artificial coverslip (Fig. 4). In agreement with the previous assay, GFP fluorescence was retained in untreated controls (Fig. 4a–f) and nisin-treated specimens (Fig. 4g–l) throughout

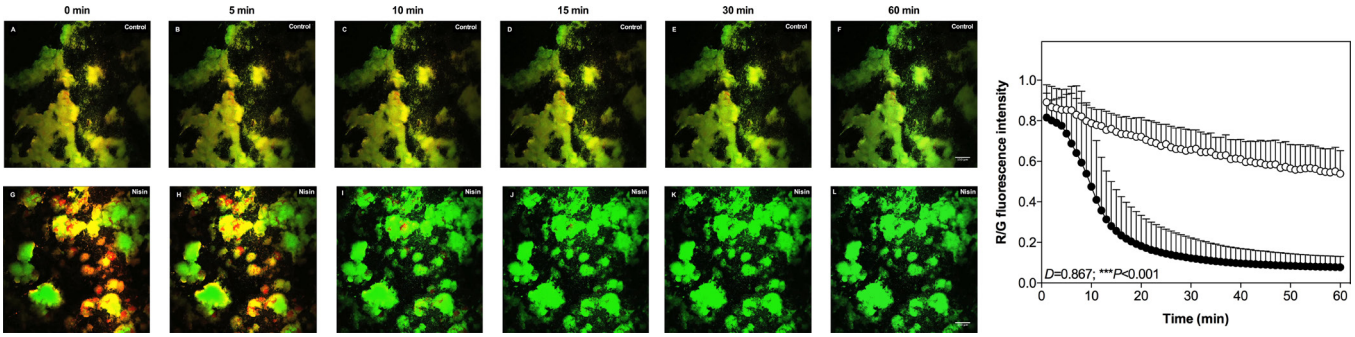

Fig. 4. Nisin flow cell treatment of *S. aureus* AH2547 CDC coverslip biofilms. Sequential images of *S. aureus* CDC coverslip biofilms under flow cell treatment in a rate of 2 ml min^{-1} at room temperature at 0, 5, 10, 15, 30 and 60 min. Control treatments were performed with phosphate buffer without nisin (a–f) and nisin treatment were performed with phosphate buffer with 15 µmol l^{-1} nisin (g–l). The GFP (green) and calcein (red) fluorescence were captured by TL-CSLM assay and the images were superimposed. The focal plane in these experiments is located near the bottom of the biofilm. Three independent evaluations were performed for each treatment and the selected images are representative for each treatment. Calcein to GFP fluorescence ratio from *S. aureus* CDC coverslip biofilms under flow cell reactor treatment were quantified using Metamorph software. Control treatment is shown in white circles and nisin treatment is shown in black circles. Fluorescence intensities were measured at 12 locations distributed randomly among the center, middle and edge zone of the biofilm. Data represent the means and sd of three replicates (only the upper limits of the error bars are represented). Calcein to GFP fluorescence ratio curves were compared by two-sample Kolmogorov–Smirnov tests (***P<0.001).

the experiment. Although some loss of red calcein fluorescence occurred under continuous flow, nisin-treated biofilms lost their red fluorescence much faster and thoroughly than the controls (Fig. 4, and Supplementary Movies 5 and 6). These observations confirmed that nisin could penetrate into the biofilm and disrupt the integrity of the cytoplasmic membrane of *S. aureus* sessile cells. Membrane permeabilization in both artificial biofilms and CDC coverslip biofilms in the flow cell reactors were quantified by the change in red (calcein) to green (GFP) fluorescence ratio and presented graphically (Figs 3 and 4). In the artificial biofilm assay, nisin-treated samples showed an average fluorescence reduction rate of 0.034 min^{-1} (85 % reduction after 60 min exposure), which was much faster (P<0.001) than untreated controls (15 % reduction after 60 min exposure). In artificial *S. aureus* biofilm exposed to nisin the fluorescence ratio decreased to half of its initial value in 28 min (Fig. 3). In the CDC coverslip biofilms, control treatments showed a gradual reduction of the fluorescence ratio (average rate of 0.053 min^{-1}) during continuous-flow treatment with approximately 17 % loss in the red to green fluorescence ratio after 15 min. In contrast, CDC coverslip biofilms treated with nisin showed a more pronounced decrease (P<0.001) in fluorescence ratio with approximately 75 % of the red to green fluorescence ratio over the same 15 min interval. When *S. aureus* CDC coverslip biofilms were exposed to nisin, fluorescence ratio decreased 50 % in 11 min (Fig. 4).

To further investigate the capacity of nisin to penetrate bacterial biofilms and affect cell viability, biofilms of *S. aureus* AH2547 were grown on CDC coupons in the CDC biofilm reactor, treated with nisin and stained with PI. Biofilm cryosection samples were analysed by confocal microscopy (Fig. 5). Cells with damaged membranes are expected to take in the red PI whereas intact cells should not. Expected morphological variations were observed among the CDC *S. aureus* biofilm specimens, such as differences in biofilm thickness and the presence or absence of robust biofilm clumps. Absence of red fluorescence was confirmed on control samples without nisin or PI staining (Fig. 5a). Additionally, as described above for planktonic cells, nisin treatment did not change the GFP fluorescence in biofilm cells (Fig. 5b). Untreated control biofilms stained with PI also showed some red fluorescence (Fig. 5c), suggesting cells lacking viability in the biofilm or naturally more permeable to PI. In contrast, most biofilm samples treated with nisin were completely stained by PI (Fig. 5d), despite the fact that variations in PI staining were observed for some nisin-treated samples (Fig. 5e). These differences may be due to cell clumping, differences in the presence of extracellular nucleic acid (eDNA) across samples [27], the existence of a subpopulation of cells in the interior of a biofilm cluster that are less susceptible to nisin or other physiological processes other than loss of membrane integrity [28]

The viability of *S. aureus* cultures in different physiological states varied when exposed to different concentrations of nisin (Fig. 6). Homogenized exponential planktonic cells (HEP) were highly susceptible to 15 μmol l^{-1} of nisin after 5 min of exposure. HEP viability decreased below the detection limit with a log reduction of at least 6.99±0.78 log c.f.u. ml^{-1}. A similar decrease in viability was observed when a tenfold higher nisin concentration was applied to HEP cells (P<0.001). Homogenized stationary planktonic cells (HSP) were much less sensitive to nisin than HEP (P<0.001). The maximum log reduction in HSP viability upon exposure to 15 μmol l^{-1} nisin was 1.64±0.50 c.f.u. ml^{-1}. Increasing nisin concentration (15 to 150 μmol l^{-1}) caused greater bactericidal activity (P<0.001) against HSP cells, with a log reduction of 3.6±0.40 c.f.u. ml^{-1}. In contrast, biofilm cultures were less susceptible to nisin than homogenized planktonic cultures. Maximum reduction in viability of homogenized biofilms (HB) and intact biofilms (IB) were always below 2 log cycles, even when cultures were exposed to 150 μmol l^{-1} nisin. Approximately 83.3 % of the sessile *S. aureus* cells were killed when the biofilm samples were treated with 15 μmol l^{-1} nisin, while a decrease of approximately 98.6 % of the viable cell number occurred at 150 μmol l^{-1} nisin.

DISCUSSION

In this work, we used a novel approach of confocal time-lapse imaging to monitor the penetration of nisin in *S. aureus* biofilms grown under continuous-flow conditions. We experimentally confirmed that this polycyclic lantibiotic causes membrane permeabilization of sessile *S. aureus* cells that are located on the bottom of the biofilm under flow treatment (Fig. 1a). We also confirmed by PI staining and *in vitro* cell viability assays that membrane integrity loss of the sessile cells correlates with a decrease in bacterial viability.

To achieve this, we used a flow cell reactor coupled with TL-CLSM to provide a direct real-time monitoring of nisin penetration through continuous-flow *S. aureus* biofilms. Biofilms were stained with an intracellular fluorescent dye (CAM) and its release was correlated with the loss of cell membrane integrity in sessile *S. aureus* cells due to the pore-forming activity of nisin (Fig. 2). Although the calcein dye used in this work is no longer commercially available from its manufacturer, it should be pointed out that other intracellular fluorescent dyes with similar properties could be used in related assays to evaluate loss for membrane integrity. To overcome the limitations of light penetration through the entire biofilm while it was being exposed to nisin, we changed the focal plane of the microscope to the bottom of the biofilm and near the coverslip interface (Fig. 1a). Therefore, in our flow cells, the deepest regions of the biofilm (i.e. the bottom of the structure), was at the top of the flow cell, against the inner side of the coverslip, providing an effective way to monitor the penetration of the peptide into the bacterial biofilm over time. This approach allowed us to monitor changes in the GFP and calcein fluorescence in the biofilm, confirming that nisin was capable to fully penetrate established biofilms and to kill sessile *S. aureus* cells. Our results also demonstrate that nisin cannot mechanically disrupt fully structured artificial or CDC biofilms even under continuous-flow treatment (Figs 3 and 4), confirming observations made for other bacterial biofilms [29].

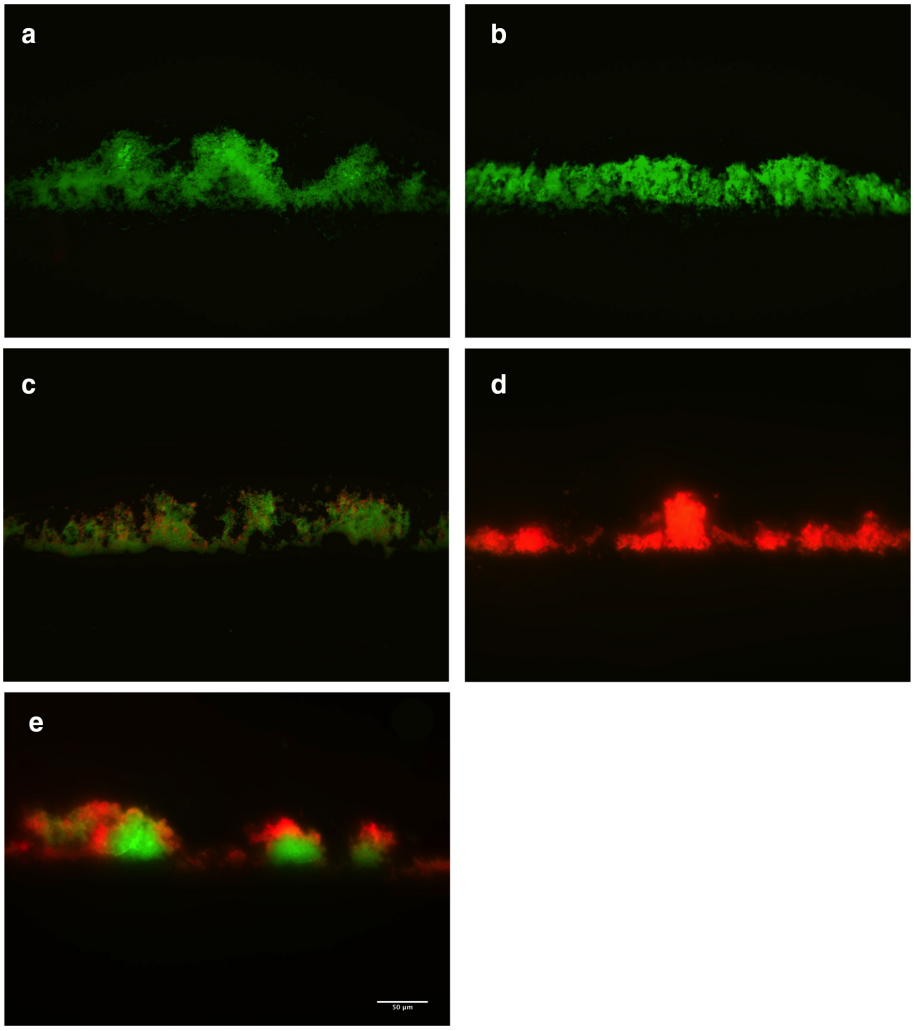

Fig. 5. Fluorescence microscopy images of *S. aureus* AH2547 CDC biofilms exposed to nisin. Before cryosectioning, *S. aureus* AH2547 CDC biofilms expressing GFP were treated with 15 µmol l^{-1} nisin during 1 h at room temperature and stained with PI. Cryosectioned biofilm samples were immobilized onto microscope slides and visualized by fluorescence microscopy (×20 magnification). The control treatments were performed with phosphate buffer without nisin: (a) Samples not stained with PI and not exposed to nisin (control 1). (b) Samples not stained with PI and exposed to nisin (control 2). (c) Samples stained with PI and not exposed to nisin (control 3). (d,e) show the *S. aureus* biofilms that were stained with PI and treated with nisin. This experiment was performed with two biological replicates and the images are representative fields for each treatment.

The artificial biofilms containing *S. aureus* cells entrapped into an inert matrix of agarose gels were much thicker than the CDC coverslip biofilms, a feature that appears to affect calcein release from the biofilm. In the artificial biofilm, calcein loss was not significant for at least 17 min after the start of the nisin treatment compared to the CDC coverslip biofilm, suggesting that the distance to the biofilm–liquid interface or the composition of the extracellular polymeric matrix slowed the speed of nisin action against sessile cells on the artificial biofilm [6]. Some decrease in calcein fluorescence was observed in control treatments, mainly in the CDC coverslip biofilms, which might due to the activity of esterases released into the extracellular matrix [30, 31]. Esterases can hydrolyse CAM in the biofilm matrix, which is followed by a subsequent loss (wash out) of the fluorescent dye in the continuous flow treatment [30–32].

Moreover, PI staining confirmed that nisin penetrates into the CDC biofilm and affects membrane permeability of sessile *S. aureus* cells (Fig. 5). PI is an intercalating agent with strong red fluorescence when bound to DNA. Because its diffusion into the cells only occurs if the cytoplasmic membrane becomes permeable, this molecule has been used as a marker to assess cell viability loss in *in vitro* killing assays [33]. Qualitative analysis of the cells stained with PI by fluorescence microscopy demonstrated that nisin-treated biofilms were more deeply stained than the controls. Nonetheless, a spatially heterogeneous PI staining was observed in the CDC

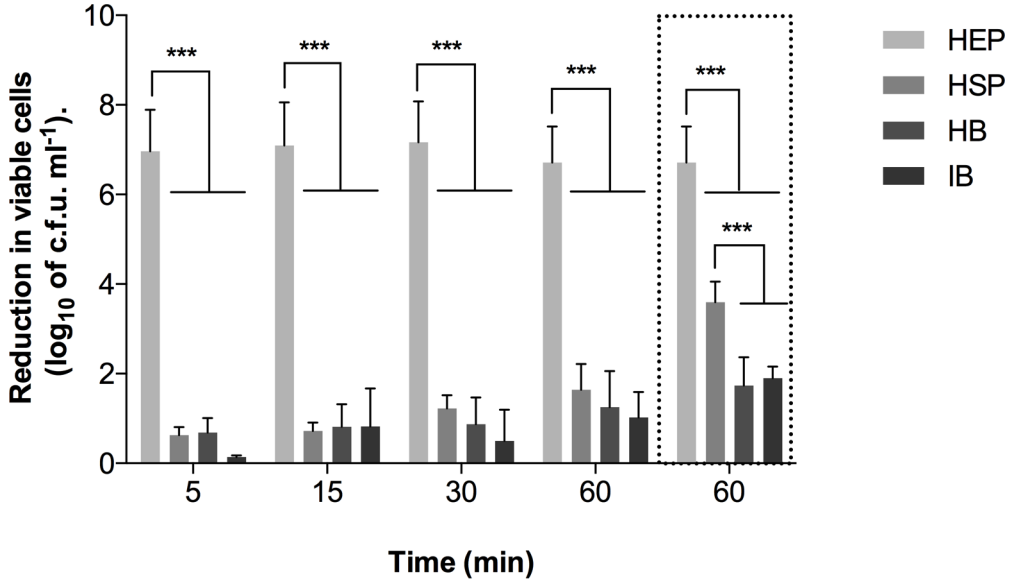

Fig. 6. Susceptibility of planktonic and sessile cells of *S. aureus* AH2547 to nisin. Nisin (15 µmol l^{-1}) was incubated with HEP cells, HSP cells, homogenized CDC biofilm (HB) and intact CDC biofilm (IB). Viabilities were determined by enumeration of c.f.u. ml^{-1} following different incubation times (0, 5, 15, 30 and 60 min). When indicated, cultures were treated with 150 µmol l^{-1} during 60 min of incubation (bars delimited by a dotted line). Control treatments were performed with phosphate buffer without nisin. The data represent the difference in viable cell number between the control and treated samples. Mean values and the SD of triplicate independent determinations are shown. Viability detection limit corresponded to 4×10^2 c.f.u. ml^{-1}. Horizontal lines above plots indicate significant differences and asterisks indicate a level of significance (***P<0.001).

biofilms when dense cell aggregates (not necessarily related to biofilm thickness) were present in nisin-treated biofilms, suggesting that factors such as variations in biofilm structure/morphology, differences in intrinsic susceptibility between cells from the interior and the periphery of the biofilms or variations in the composition of the extracellular polymeric matrix affect PI uptake or the efficacy of nisin to diffuse into the interior of the biofilm.

Biofilms show great physiological heterogeneity, but most sessile cells have slow growth rates and low cell-wall turnover rates [5, 34]. Therefore, alterations in the availability of target molecules (lipid II) could potentially affect the sensitivity to nisin. Lipid II is essential to transport peptidoglycan monomers during cell-wall biosynthesis [35, 36] and a dramatic efflux of cytoplasmic compounds is induced when nisin–lipid II complexes form in the cytoplasmic membrane, causing membrane depolarization and consequent cellular death [37]. Specific interactions between nisin and lipid II also prevent the incorporation of newly synthesized glycan chains into the existing sacculus, thus inhibiting cell-wall biosynthesis and increasing its inhibitory effect [35, 38]. Additionally, cell-wall biosynthesis in *S. aureus* occurs predominantly at the division septum, which is rich in lipid II [39, 40]. This uneven distribution of lipid II could also affect nisin efficiency [17, 41, 42]. In a previous study, telavancin, a semisynthetic derivative of vancomycin with high affinity to lipid I, bound mostly to lipid II placed in the division septum of exponentially growing *S. aureus* cells, thus causing efficient membrane depolarization [40].

Because direct evaluation confirmed that nisin is able to penetrate *S. aureus* biofilms and damage *S. aureus* sessile cells, the variation in nisin susceptibility appears to be mainly related to phenotypic (physiological) differences between the sessile and planktonic cultures. Although biofilms formed under flow conditions by clinically relevant micro-organisms have physical and chemical features similar to natural biofilms in invasive devices, we did not observe significant interactions between nisin and the *S. aureus* extracellular matrix. Despite having molecular weight at least an order of magnitude higher than common biocides (e.g. quaternary ammonium compounds – QAC), it was previously shown that nisin could traverse the stratified layers of *S. epidermidis* biofilms faster than QACs [29]. Nisin also shows superior bactericidal activity against biofilm cells compared to Nukacin ISK-1, a lantibiotic produced by *Staphylococcus warneri* ISK-1, and Lacticin Q, a class IId bacteriocin produced by *Lactococcus lactis* QU 5 [11]. Taken together, these observations indicate that there are variations in the antibiofilm activity of membrane-depolarizing antimicrobial peptides and killing efficacy could be related to the biofilm penetration time and potential sorption to the biofilm matrix. Therefore, strategies such as the association of nisin with compounds that are effective eradicating biofilms (e.g. tetrasodium EDTA), quorum sensing

inhibitors (e.g. colostrum hexasaccharide) [43] or its use against immature (thinner) biofilms could improve the bactericidal activity against sessile cells of *S. aureus*.

Conclusions

We provide real-time evidence through direct microscopic visualization in flow conditions that nisin is able to penetrate into the interior of continuous-flow *S. aureus* biofilms and kill sessile cells of this relevant human and animal pathogen. Also, the similarities in sensitivity of HSP and HB cells to nisin reinforce the complex relevance interplay between the physiology of bacteria and the sensitivity to antimicrobials. Based on evidence that biofilms show a wide array of resistance mechanisms, our new approach to assess biofilm susceptibility could improve the evaluation of susceptibility breakpoints of promising antimicrobials. Over the years, a combination of traditional techniques and confocal microscopy has promoted significant advances in the field and further investigations using the continuous flow cell reactor could provide more feasible assessments of the therapeutic effects of antimicrobial agents against sessile cells of clinically relevant pathogens under continuous-flow conditions.

Funding information
This work was supported by the Fundação de Amparo a Pesquisa do Estado de Minas Gerais (FAPEMIG; Belo Horizonte, Brazil), Coordenação de Aperfeiçoamento de Pessoal de Nível Superior (CAPES; Brasília, Brazil) and INCT Ciência Animal. F. G. S. received a fellowship from the Conselho Nacional de Desenvolvimento Científico e Tecnológico (CNPq; Brasília, Brazil). Microscopy at the Center for Biofilm Engineering was made possible by awards from the Murdock Charitable Trust and the National Science Foundation (CBET 1039785).

Acknowledgements
The authors would like to thank the anonymous reviewers for their constructive criticisms and valuable comments that helped improve the final version of the manuscript

Conflicts of interest
The authors declare that there are no conflicts of interest.

References

1. C.D.C. 2018. Centre for disease prevention and control: C.D.C. Available from. http://www.cdc.gov/HAI/surveillance/index.html [accessed cited 2018 12/12].
2. Peton V, Le Loir Y. *Staphylococcus aureus* in veterinary medicine. *Infect Genet Evol* 2014;21:602–615.
3. Tong SYC, Davis JS, Eichenberger E, Holland TL, Fowler VG. *Staphylococcus aureus* infections: epidemiology, pathophysiology, clinical manifestations, and management. *Clin Microbiol Rev* 2015;28:603–661.
4. Bjarnsholt T. The role of bacterial biofilms in chronic infections. *APMIS* 2013;121:1–58.
5. Hall CW, Mah T-F. Molecular mechanisms of biofilm-based antibiotic resistance and tolerance in pathogenic bacteria. *FEMS Microbiol Rev* 2017;41:276–301.
6. Stewart PS, biofilms Din. Diffusion in biofilms. *J Bacteriol* 2003;185:1485–1491.
7. Aggarwal S, Stewart PS, Hozalski RM. Biofilm cohesive strength as a basis for biofilm recalcitrance: are bacterial biofilms overdesigned? *Microbiol Insights* 2015;8s2:MBI.S31444–32.
8. Conlon BP. *Staphylococcus aureus* chronic and relapsing infections: Evidence of a role for persister cells: An investigation of persister cells, their formation and their role in *S. aureus* disease. *Bioessays* 2014;36:991–996.
9. Costerton JW, Stewart PS, Greenberg EP. Bacterial biofilms: a common cause of persistent infections. *Science* 1999;284:1318–1322.
10. Le Lay C, Dridi L, Bergeron MG, Ouellette M, Fliss IL, Lay CL, Il F. Nisin is an effective inhibitor of *Clostridium difficile* vegetative cells and spore germination. *J Med Microbiol* 2016;65:169–175.
11. Okuda K-ichi, Zendo T, Sugimoto S, Iwase T, Tajima A *et al*. Effects of bacteriocins on methicillin-resistant *Staphylococcus aureus* biofilm. *Antimicrob Agents Chemother* 2013;57:5572–5579.
12. Pimentel-Filho NdeJ, Mantovani HC, de Carvalho AF, Dias RS, Vanetti MCD. Efficacy of bovicin HC5 and nisin combination against *Listeria monocytogenes* and *Staphylococcus aureus* in fresh cheese. *Int J Food Sci Technol* 2014;49:416–422.
13. Paiva AD, de Oliveira MD, de Paula SO, Baracat-Pereira MC, Breukink E *et al*. Toxicity of bovicin HC5 against mammalian cell lines and the role of cholesterol in bacteriocin activity. *Microbiology* 2012;158:2851–2858.
14. Shin JM, Gwak JW, Kamarajan P, Fenno JC, Rickard AH *et al*. Biomedical applications of nisin. *J Appl Microbiol* 2016;120:1449–1465.
15. Breukink E, Wiedemann I, van Kraaij C, Kuipers OP, Sahl HG *et al*. Use of the cell wall precursor lipid II by a pore-forming peptide antibiotic. *Science* 1999;286:2361–2364.
16. F.D.A. Nisin preparation: affirmation of GRAS status as a direct human food ingredient. *Fed Regist* 1988;53:11247–11251.
17. Breukink E, van Heusden HE, Vollmerhaus PJ, Swiezewska E, Brunner L *et al*. Lipid II is an intrinsic component of the pore induced by nisin in bacterial membranes. *J Biol Chem* 2003;278:19898–19903.
18. Ceotto-Vigoder H, Marques SLS, Santos INS, Alves MDB, Barrias ES *et al*. Nisin and lysostaphin activity against preformed biofilm of *Staphylococcus aureus* involved in bovine mastitis. *J Appl Microbiol* 2016;121:101–114.
19. Otto M. Staphylococcal biofilms. *Curr Top Microbiol Immunol* 2008;322:207–228.
20. Bjarnsholt T, Ciofu O, Molin S, Givskov M, Høiby N. Applying insights from biofilm biology to drug development - can a new approach be developed? *Nat Rev Drug Discov* 2013;12:791–808.
21. Herbert S, Ziebandt A-K, Ohlsen K, Schäfer T, Hecker M *et al*. Repair of global regulators in *Staphylococcus aureus* 8325 and comparative analysis with other clinical isolates. *Infect Immun* 2010;78:2877–2889.
22. Gilcreas FW. Standard methods for the examination of water and waste water. *Am J Public Health Nations Health* 1966;56:387–388.
23. C.L.S.I. *M100-S23 Performance standards for antimicrobial susceptibility testing*, twenty-third informational supplement. Wayne, PA, USA: Clinical and Laboratory Standards Institute; 2013.
24. C.B.E. CDC biofilm reactor operator's manual. *Center for Biofilm Engineering-Montana State University*. Bozeman, MT: Montana State University; 2003.
25. FP Y, Callis GM, Stewart PS, Griebe T, McFeters GA. Cryosectioning of biofilms for microscopic examination. *Biofouling* 1994;8:85–91.
26. Miles AA, Misra SS, Irwin JO. The estimation of the bactericidal power of the blood. *J Hyg* 1938;38:732–749.
27. Rosenberg M, Azevedo NF, Ivask A. Propidium iodide staining underestimates viability of adherent bacterial cells. *bioRxiv* 2018;475145.
28. Yang Y, Xiang Y, Xu M. From red to green: the propidium iodide-permeable membrane of *Shewanella decolorationis* S12 is repairable. *Sci Rep* 2016;5:18583–18583.
29. Davison WM, Pitts B, Stewart PS. Spatial and temporal patterns of biocide action against *Staphylococcus epidermidis* biofilms. *Antimicrob Agents Chemother* 2010;54:2920–2927.
30. Foulston L, Elsholz AKW, DeFrancesco AS, Losick R. The extracellular matrix of *Staphylococcus aureus* biofilms comprises

cytoplasmic proteins that associate with the cell surface in response to decreasing pH. *MBio* 2014;5:e01667–01614.

31. Jachlewski S, Jachlewski WD, Linne U, Bräsen C, Wingender J *et al*. Isolation of extracellular polymeric substances from biofilms of the thermoacidophilic archaeon *Sulfolobus acidocaldarius*. *Front Bioeng Biotechnol* 2015;3:123.
32. Pasztor L, Ziebandt A-K, Nega M, Schlag M, Haase S *et al*. Staphylococcal major autolysin (ATL) is involved in excretion of cytoplasmic proteins. *J Biol Chem* 2010;285:36794–36803.
33. Stiefel P, Schmidt-Emrich S, Maniura-Weber K, Ren Q. Critical aspects of using bacterial cell viability assays with the fluorophores SYTO9 and propidium iodide. *BMC Microbiol* 2015;15:36–39.
34. Folsom JP, Richards L, Pitts B, Roe F, Ehrlich GD *et al*. Physiology of *Pseudomonas aeruginosa* in biofilms as revealed by transcriptome analysis. *BMC Microbiol* 2010;10:294.
35. Wiedemann I, Breukink E, van Kraaij C, Kuipers OP, Bierbaum G *et al*. Specific binding of nisin to the peptidoglycan precursor lipid II combines pore formation and inhibition of cell wall biosynthesis for potent antibiotic activity. *J Biol Chem* 2001;276:1772–1779.
36. de Kruijff B, van Dam V, Breukink E. Lipid II: a central component in bacterial cell wall synthesis and a target for antibiotics. *Prostaglandins Leukot Essent Fatty Acids* 2008;79:117–121.
37. Tol MB, Morales Angeles D, Scheffers D-J. *In* vivo cluster formation of nisin and lipid II is correlated with membrane depolarization. *Antimicrob Agents Chemother* 2015;59:3683–3686.
38. Wiedemann I, Benz R, Sahl H-G. Lipid II-mediated pore formation by the peptide antibiotic nisin: a black lipid membrane study. *J Bacteriol* 2004;186:3259–3261.
39. Pinho MG, Errington J. Dispersed mode of *Staphylococcus aureus* cell wall synthesis in the absence of the division machinery. *Mol Microbiol* 2003;50:871–881.
40. Lunde CS, Rexer CH, Hartouni SR, Axt S, Benton BM. Fluorescence microscopy demonstrates enhanced targeting of telavancin to the division septum of *Staphylococcus aureus*. *Antimicrob Agents Chemother* 2010;54:2198–2200.
41. Prince A, Sandhu P, Ror P, Dash E, Sharma S *et al*. Lipid-II independent antimicrobial mechanism of nisin depends on its crowding and degree of oligomerization. *Scientific Reports* 2016;6:37908.
42. Bierne H, Dramsi S. Spatial positioning of cell wall-anchored virulence factors in Gram-positive bacteria. *Curr Opin Microbiol* 2012;15:715–723.
43. Srivastava A, Singh BN, Deepak D, Rawat AKS, Singh BR. Colostrum hexasaccharide, a novel *Staphylococcus aureus* quorum-sensing inhibitor. *Antimicrob Agents Chemother* 2015;59:2169–2178.

Edited by: J. Stülke and M. Vickerman